Available online at www.sciencedirect.com
SCIENCE DIRECT
International Journal of Solids and Structures 43 (2006) 3213–3229
INTERNATIONAL JOURNAL OF SOLIDS and STRUCTURES
www.elsevier.com/locate/ijsolstr

Thermoelastic damping in micro-beam resonators

Yuxin Sun [a], Daining Fang [a,*], Ai Kah Soh [b]

[a] Department of Engineering Mechanics, Tsinghua University, Beijing 100084, PR China
[b] Department of Mechanical Engineering, University of Hong Kong, Hong Kong, PR China

Received 13 February 2005
Available online 5 October 2005

Abstract

Thermoelastic damping is recognized as a significant loss mechanism at room temperature in micro-scale beam resonators. In this paper, the governing equations of coupled thermoelastic problems are established based on the generalized thermoelastic theory with one relaxation time. The thermoelastic damping of micro-beam resonators is analyzed by using both the finite sine Fourier transformation method combined with Laplace transformation and the normal mode analysis. The vibration responses of deflection and thermal moment are obtained for the micro-beams with simply supported and isothermal boundary conditions. The vibration frequency is analyzed for three boundary condition cases, i.e., the clamped and isothermal, the simply supported and isothermal, and the simply supported and adiabatic. The analytic results show that the amplitude of deflection and thermal moment are attenuated and the vibration frequency is increased with thermoelastic coupling effect being considered. In addition, it can be found from both the analytic results and the numerical calculations that these properties are size-dependent. When the thickness of the micro-beam is larger than its characteristic size, the effect of thermoelastic damping weakens as the beam thickness increases. The size-effect induced by thermoelastic coupling would disappear when the thickness of the micro-beam is over a critical value that depends on the material properties and the boundary conditions.

Keywords: Thermoelastic damping; Micro-scale beam resonator; Integration transformation; Generalized thermoelastic theory

1. Introduction

Micro-scale mechanical resonators have high sensitivity as well as fast response (Barnes et al., 1994; Stowe et al., 1996; Mihailovich and Parpia, 1992; Yurke et al., 1995) and are widely used as sensors and modulators (Tang et al., 1990; Mihailovich and MacDonald, 1995; Tortonese et al., 1993; Zook et al., 1996; Burns et al., 1995; Cleland and Roukes, 1996, 1999). It is necessary to know how the parameters affect their physical properties and mechanical properties. For resonators, it is desired to design and construct systems with loss of energy as little as possible. Unfortunately, it has been consistently observed that there exists energy dissipation that increases with size decreasing significantly—even when made from pure single-crystal materials (Lifshitz

* Corresponding author.
E-mail address: fangdn@mail.tsinghua.edu.cn (D. Fang).

0020-7683/$ - see front matter © 2005 Elsevier Ltd. All rights reserved.
doi:10.1016/j.ijsolstr.2005.08.011

and Roukes, 2000). Many researchers have discussed different dissipation mechanisms in MEMS (Akhiezer and Berestetskii, 1965; Hosaka et al., 1995; Tilmans et al., 1992; Mihailovich and MacDonald, 1995; Zhang et al., 2003; Carr et al., 1998; Harrington et al., 2000; Zener, 1937, 1938), such as doping impurities losses, support-related losses, thermoelastic damping, and the Akhiezer effect (Akhiezer and Berestetskii, 1965), as well as the radiation of energy away from the resonator into its surroundings. Mihailovich and MacDonald (1995) measured the mechanical loss of various micron-sized vacuum-operated single-crystal silicon resonators, to identify their dominant loss mechanism. They examined three possible sources of mechanical loss, including doping-impurity losses, support-related losses and surface-related losses. Zhang et al. (2003) studied the effect of air damping on the frequency response and the quality factor of a micro-machined beam resonator. Their results indicate that air damping generally shifts the resonance frequency on the order of no more than 10^{-6} and degrades the quality factor, and that this effect of air damping increases as the dimension of the beam decreases. Harrington et al. (2000) measured mechanical dissipation in micron-sized single-crystal gallium arsenide resonators that vibrate in torsion and flexural modes. They found that the resonance frequency changes with temperature.

It has been verified that thermoelastic damping is a significant loss mechanism near room temperature in MEMS resonators. Zener (1937) predicted the existence of the thermoelastic damping process and then quickly verified the basic aspects of the theory experimentally. Further experiments consistent with Zener's theory were provided by Berry (1955) for α-brass. In the case the damping was measured as a function of frequency at room temperature. Roszhardt (1990) observed thermoelastic damping in single-crystal silicon micro-resonators at room temperature; and Yasumura et al. (1999) also reported thermoelastic damping in silicon nitride micro-resonators at room temperature, but their measured results are an order of magnitude smaller than Roszhart's.

Thermoelastic vibration of beams has been widely investigated. Landau and Lifshitz (1959) provided an exact expression for the attenuation coefficient of thermoelastic vibration, but they did not give a rigorous derivation and solution of the governing equations. Massalas and Kalpakiclis (1983) analyzed the vibration of a beam whose surface is subjected to a step heat flux. But they ignored the inertia item in order to make a simplification. Givoli and Rand (1995) studied the effect of thermoelastic coupling on dynamic response properties of a rod. They found that when the frequency of the thermal loading is close to the critical frequency of the rod, the nature of the dynamic response of the structure is changed significantly. Boley (1972) analyzed the thermally induced vibrations of a simply supported rectangular beam. Manolis and Beskos (1980) studied the effect of damping and axial loads on the vibration of beams induced by fast heating on the surface. They also considered the effect of damping and axial loading, but disregarded the coupling between stress and temperature fields. Copper and Pilkey (2002) presented a thermoelastic solution technique for beams with arbitrary quasi-static temperature distributions that create large transverse normal and shear stresses. They calculated the stress resultants and midspan displacements along a beam. Houston et al. (2004) studied the importance of thermoelastic damping for silicon-based MEMS. Their results indicate that the internal friction arising from this mechanism is strong and persists down to 50 nm scale structures.

Up to date, a little of work relative to the size effect of thermoelastic damping upon vibration frequency response for the micro-resonators has been reported. Guo and Rogerson (2003) studied the thermoelastic coupling in a doubly clamped elastic prism beam and examined its size-dependence. Lifshitz and Roukes (2000) studied thermoelastic damping of a beam with rectangular cross-sections, and found that after the Debye peaks, the thermoelastic attenuation will be weakened as the size increases. However, the results of both Guo and Rogerson (2003) and Lifshitz and Roukes (2000) were obtained based on the classical Fourier thermal conducting equation and the effect of boundary conditions were not considered in their work.

From the above summary, it can be concluded that first the above-mentioned investigations were based on the classical thermoelastic theory, assuming the infinite speed of heat transportation. Second, the effect of different boundary conditions such as mechanical supporting and heat transferring conditions at the ends of beams were not taken into consideration. Third, studying the size effect of thermoelastic damping upon vibration frequency response for the micro-resonators is insufficient, especially for the analysis based on the generalized thermoelastic theory with non-Fourier thermal conduction equations. In this paper, the governing equations of coupled thermoelastic problems are established based on the generalized thermoelastic theory with one relaxation time. The thermoelastic damping of micro-beam resonators are analyzed by using both

the finite sine Fourier transformation method combined with Laplace transformation and the normal mode analysis (Ezzat et al., 2001). The vibration frequency response is analyzed for three boundary condition cases, i.e., the clamped and isothermal, the simply supported and isothermal, and the simply supported and adiabatic. A particular attention is paid to the size dependency of thermoelastic damping.

2. Description of thermoelastic damping

An elastic wave dissipates energy due to intrinsic and extrinsic mechanisms. Some of the extrinsic mechanisms are affected by changes of environment; for example, air damping can be minimized under ultrahigh-vacuum (UHV) conditions. The intrinsic dissipation mechanism can be regarded as phonon–phonon interaction, namely the scattering of acoustic phonons with thermal phonons (Lifshitz and Roukes, 2000).

When an elastic solid is set in motion, it is taken out of equilibrium, having an excess of kinetic and potential energy. The coupling of the strain field to a temperature field provides an energy dissipation mechanism that allows the system to relax back to equilibrium. This process of energy dissipation, called thermoelastic damping, is what we will discuss in this paper.

Zener (1937, 1938) firstly studied the transverse vibration of thin reeds and developed the thermoelastic damping theory. Thermoelastic damping arises from thermal currents generated by compression/decompression in elastic media. The bending of the reed causes dilations of opposite signs to exist on the upper and lower halves. One side is compressed and heated, and the other side is stretched and cooled. Thus, in the presence of finite thermal expansion, a transverse temperature gradient is produced. The temperature gradient generates local heat currents, which cause increase of the entropy of the reed and lead to energy dissipation. The temperature across the reed equalizes in a characteristic time τ_R, while the flexural period of the reed is ω^{-1} (ω is the vibration frequency of the reed). In the low-frequency range, i.e., $\tau_R \ll \omega^{-1}$, the vibrations are isothermal and a small amount of energy is dissipated. On the other hand, for $\tau_R \gg \omega^{-1}$, adiabatic conditions prevail with low-energy dissipation similar to the low-frequency range. While $\tau_R \approx \omega^{-1}$, stress and strain are out of phase and a maximum of internal friction occurs. This is the so-called Debye peak. For a beam of thickness, h, with a rectangular cross-section, its characteristic time is

$$\tau_R(T) = (h/\pi)^2 D^{-1}(T), \tag{1}$$

where T is the temperature of the beam and $D = k/\rho c_v$, the thermal diffusion coefficient, in which ρ, k and c_v are the density, thermal conductivity and specific heat at constant volume, respectively. The vibration frequency of a reed is

$$\omega = \frac{q^2 h}{L^2}\sqrt{\frac{E}{12\rho}}, \tag{2}$$

where E is the Young's modulus; L, the beam length, and the allowed values of q are determined by the supporting conditions at the two ends of the beam. For beams with both ends clamped $q = 4.73$, while $q = \pi$ for beams with both ends simply supported.

In Zener's theory (1937, 1938), the classical Fourier thermal conduction theory is applied and there is no heat flow perpendicular to the surfaces of the beam. Thus, the internal friction, Q^{-1} (Q is the quality factor defined by Zener, 1937), is defined as follows:

$$Q^{-1} = \frac{\alpha_T^2 TE}{C_p}\frac{\omega\tau_R}{1+\omega^2\tau_R^2}, \tag{3}$$

where C_p is the specific heat at constant pressure; α_T, the coefficient of linear thermal expansion; T, the temperature of the reed and ω and τ_R are defined in Eqs. (1) and (2).

Lifshitz and Roukes (2000) gave another expression for the thermoelastic damping by

$$Q^{-1} = \frac{\alpha_T^2 TE}{C_p}\left(\frac{6}{\xi^2} - \frac{6}{\xi^3}\frac{\sinh\xi + \sin\xi}{\cosh\xi + \cos\xi}\right) \tag{4}$$

in which $\xi = h\sqrt{\omega/2D}$.

Note that Zener used the classical thermoelastic theory assuming infinite speed of heat transportation. While this paper uses the generalized thermoelastic theory with the non-Fourier thermal conduction equation to modify Zener's theory.

In Zener's study, the size of the beam was fixed and the two ends of the beams were clamped. In this paper the effect of both the beam size and the mechanical and thermal boundary conditions at the two ends are taken into consideration.

3. Formulation of basic equations

Beams with rectangular cross-sections are mostly employed in MEMS resonators. A micro-resonator can be modeled as an elastic prism beam with either doubly clamped or simply supported ends. Here we consider small flexural deflections of a thin elastic beam with dimensions of length L ($0 \leqslant x \leqslant L$), width b ($-b/2 \leqslant y \leqslant b/2$) and thickness h ($-h/2 \leqslant z \leqslant h/2$). We define the x axis along the axis of the beam and the y and z axes correspond to the width and thickness, respectively. In equilibrium, the beam is unstrained, unstressed, and at temperature T_0 everywhere. There is no flow of heat across the upper and lower surfaces of the beam so that $\partial\theta/\partial z = 0$ at $z = \pm h/2$.

The usual Euler–Bernoulli assumption is made so that any plane cross-section, initially perpendicular to the axis of the beam, remains plane and perpendicular to the neutral surface during bending. Thus, the displacements can be given by

$$u = -z\frac{\mathrm{d}w}{\mathrm{d}x}, \quad v = 0, \quad w(x,y,z,t) = w(x,t), \tag{5}$$

where t is time. The one-dimensional constitutive equation is

$$\sigma_x = -Ez\frac{\partial^2 w}{\partial x^2} - \beta\theta, \tag{6}$$

where E is the Young's modulus; $\theta = T - T_0$, the temperature increment of the resonator; and $\beta = E\alpha_{\mathrm{T}}/(1-2v)$ the thermal modulus in which α_{T} is the coefficient of linear thermal expansion and v, the Poison's ratio. Then the flexure moment of the cross-section is given as follows:

$$M(x,t) = -\int_{-\frac{h}{2}}^{\frac{h}{2}} b\sigma_x z\,\mathrm{d}z = EI\frac{\partial^2 w}{\partial x^2} + b\beta\int_{-\frac{h}{2}}^{\frac{h}{2}} \theta z\,\mathrm{d}z, \tag{7}$$

where $I = bh^3/12$ is the inertia moment of the cross-section. If the thermal moment, $M_{\mathrm{T}} = b\beta\int_{-\frac{h}{2}}^{\frac{h}{2}}\theta z\,\mathrm{d}z$, is denoted, Eq. (7) can be rewritten as

$$M(x,t) = EI\frac{\partial^2 w}{\partial x^2} + M_{\mathrm{T}}. \tag{8}$$

The equation of transverse motion for a beam is

$$\frac{\partial^2 M}{\partial x^2} + \rho A\frac{\partial^2 w}{\partial t^2} = 0, \tag{9}$$

where ρ is the density; $A = bh$, the cross-section area; and EI, the flexural rigidity of the beam.

Substituting Eq. (8) into Eq. (9), we can get the motion equation of the beam as follows:

$$EI\frac{\partial^4 w}{\partial x^4} + \frac{\partial^2 M_{\mathrm{T}}}{\partial x^2} + \rho A\frac{\partial^2 w}{\partial t^2} = 0. \tag{10}$$

The non-Fourier thermal conduction equation containing the thermoelastic coupling term has the following form:

$$k\theta_{,ii} = \rho c_v\frac{\partial\theta}{\partial t} + \beta T_0\frac{\partial u_{i,i}}{\partial t} + \tau_0\rho c_v\frac{\partial^2\theta}{\partial t^2} + \tau_0\beta T_0\frac{\partial^2 u_{i,i}}{\partial t^2}, \tag{11}$$

where T_0 is the reference temperature; c_v, the specific heat at constant volume; τ_0, the thermal relaxation time; and k, the thermal conductivity.

Substituting the Euler–Bernoulli assumption, namely Eq. (5), into Eq. (11) gives the thermal conduction equation for the beam,

$$k\frac{\partial^2\theta}{\partial x^2}+k\frac{\partial^2\theta}{\partial z^2}=c_v\rho\frac{\partial\theta}{\partial t}-T_0\beta z\frac{\partial^3 w}{\partial x^2\,\partial t}+\tau_0 c_v\rho\frac{\partial^2\theta}{\partial t^2}-\tau_0 T_0\beta z\frac{\partial^4 w}{\partial x^2\,\partial t^2}. \tag{12}$$

Multiplying Eq. (12) by means of $b\beta z$ and integrating it with respect to z from $-h/2$ to $h/2$, yield

$$k\frac{\partial^2 M_T}{\partial x^2}+k\int_{-\frac{h}{2}}^{\frac{h}{2}}b\beta z\frac{\partial^2\theta}{\partial z^2}\,\mathrm{d}z-c_v\rho\frac{\partial M_T}{\partial t}+T_0\beta^2 I\frac{\partial^3 w}{\partial x^2\,\partial t}-\tau_0 c_v\rho\frac{\partial^2 M_T}{\partial t^2}+\tau_0 T_0\beta^2 I\frac{\partial^4 w}{\partial x^2\,\partial t^2}=0. \tag{13}$$

For a very thin beam, assuming that the temperature increment varies in terms of a $\sin(pz)$ function along the thickness direction, where $p=\frac{\pi}{h}$, gives

$$M_T=b\beta\int_{-\frac{h}{2}}^{\frac{h}{2}}\theta z\,\mathrm{d}z=\frac{b\beta}{p^2}\left[\theta|_{-h/2}^{h/2}-z\frac{\partial\theta}{\partial z}\Big|_{-h/2}^{h/2}\right]=-\frac{1}{p^2}\int_{-\frac{h}{2}}^{\frac{h}{2}}b\beta\frac{\partial^2\theta}{\partial z^2}z\,\mathrm{d}z. \tag{14}$$

Substituting Eq. (14) into Eq. (13), leads to

$$k\frac{\partial^2 M_T}{\partial x^2}-kp^2M_T-c_v\rho\frac{\partial M_T}{\partial t}+T_0\beta^2 I\frac{\partial^3 w}{\partial x^2\,\partial t}-\tau_0 c_v\rho\frac{\partial^2 M_T}{\partial t^2}+\tau_0 T_0\beta^2 I\frac{\partial^4 w}{\partial x^2\,\partial t^2}=0. \tag{15}$$

Now the governing equations for the coupled thermoelastic problem can be obtained as follows:

$$\begin{cases} EI\dfrac{\partial^4 w}{\partial x^4}+\dfrac{\partial^2 M_T}{\partial x^2}+\rho A\dfrac{\partial^2 w}{\partial t^2}=0, \\ k\dfrac{\partial^2 M_T}{\partial x^2}-kp^2M_T-c_v\rho\dfrac{\partial M_T}{\partial t}+T_0\beta^2 I\dfrac{\partial^3 w}{\partial x^2\,\partial t}-\tau_0 c_v\rho\dfrac{\partial^2 M_T}{\partial t^2}+\tau_0 T_0\beta^2 I\dfrac{\partial^4 w}{\partial x^2\,\partial t^2}=0. \end{cases} \tag{16}$$

The following dimensionless quantities are defined to transform Eq. (16) into non-dimensional form:

$$\xi=\frac{x}{L},\quad W=\frac{w}{h},\quad \tau=\frac{t\varepsilon}{L},\quad \varepsilon=\sqrt{\frac{E}{\rho}},\quad \Theta=\frac{M_T}{EAh}, \tag{17}$$

where W is the dimensionless deflection and Θ, the dimensionless thermal moment. Then Eq. (16) becomes

$$\begin{cases} \dfrac{\partial^2 W}{\partial\tau^2}+A_1\dfrac{\partial^4 W}{\partial\xi^4}+\dfrac{\partial^2\Theta}{\partial\xi^2}=0, \\ \dfrac{\partial^2\Theta}{\partial\xi^2}-A_2\Theta-A_3\dfrac{\partial\Theta}{\partial\tau}+A_4\dfrac{\partial^3 W}{\partial\xi^2\,\partial\tau}-A_5\dfrac{\partial^2\Theta}{\partial\tau^2}+A_6\dfrac{\partial^4 W}{\partial\xi^2\,\partial\tau^2}=0. \end{cases} \tag{18}$$

The coefficients in Eq. (18) are

$$A_1=\frac{h^2}{12L^2},\quad A_2=p^2L^2,\quad A_3=\frac{c_v\rho\varepsilon L}{k},\quad A_4=\frac{T_0\beta^2h^2\varepsilon}{12kEL},\quad A_5=\frac{\tau_0 c_v E}{k},\quad A_6=\frac{\tau_0 T_0\beta^2h^2}{12\rho kL^2}. \tag{19}$$

If the thermoelastic coupling effect is disregarded, the governing equations consisting of the non-Fourier thermal conduction equation and the motion equation of the beam can be expressed as

$$\begin{cases} k\dfrac{\partial^2\theta}{\partial x^2}+k\dfrac{\partial^2\theta}{\partial z^2}=\rho c_v\dfrac{\partial\theta}{\partial t}+\tau_0\rho c_v\dfrac{\partial^2\theta}{\partial t^2}, \\ EI\dfrac{\partial^4 w}{\partial x^4}+\rho A\dfrac{\partial^2 w}{\partial t^2}=0. \end{cases} \tag{20}$$

Comparing Eq. (16) with Eq. (20) shows that it is much more difficult to solve the governing equation of the coupled thermoelastic case than to solve that of the uncoupled case.

4. Solutions and results

It is challenging to solve the governing equations considering the thermoelastic coupling effect (i.e., Eq. (18)). In this paper, two methods are used to analyze the thermoelastic coupling effect of the micro-beam resonators. Firstly, the integration transformation method is employed to solve Eq. (18) for micro-beams with two simply supported and isothermal ends. In this case, the damping characteristics of deflection and thermal moment vibration are analyzed. Secondly, the normal mode analysis is used to solve Eq. (18) for micro-beams with different supporting and heat transferring boundary conditions at the two beam-ends. The vibration frequency response is analyzed for three boundary-condition cases, such as the clamped and isothermal, the simply supported and isothermal, and the simply supported and adiabatic. In addition, the results obtained by using the normal mode analysis are compared with the numerical results based on the finite difference method. The analysis and discussion is emphasized particularly on the size effect of thermoelastic damping.

4.1. Analysis based on integration transformation method

When the two ends of the micro-beams are simply supported and held at a constant temperature, the boundary conditions are given by

$$\begin{cases} W|_{\xi=0} = W|_{\xi=1} = 0, \\ \left.\dfrac{\partial^2 W}{\partial \xi^2}\right|_{\xi=0} = \left.\dfrac{\partial^2 W}{\partial \xi^2}\right|_{\xi=1} = 0, \\ \Theta|_{\xi=0} = \Theta|_{\xi=1} = 0. \end{cases} \tag{21}$$

To solve Eq. (18), a finite sine Fourier transformation can be used:

$$\begin{cases} W_m(m,\tau) = \int_0^1 W(\xi,\tau)\sin(r_m\xi)\,\mathrm{d}\xi, \\ \Theta_m(m,\tau) = \int_0^1 \Theta(\xi,\tau)\sin(r_m\xi)\,\mathrm{d}\xi, \end{cases} \tag{22}$$

where $r_m = m\pi$, $m = 1,3,5\ldots$

The solutions of Eq. (22) automatically satisfy to the boundary conditions (i.e., Eq. (21)). Based on the Fourier series theory, the inverse transformation towards Eq. (22) can be expressed by

$$\begin{cases} W(\xi,\tau) = 2\sum\limits_{m=1,3,\ldots}^{\infty} W_m(m,\tau)\sin(r_m\xi), \\ \Theta(\xi,\tau) = 2\sum\limits_{m=1,3,\ldots}^{\infty} \Theta_m(m,\tau)\sin(r_m\xi). \end{cases} \tag{23}$$

In a case that a uniform force, F, is applied on the upper surface of the beam, the initial conditions can be set as follows:

$$\begin{cases} W|_{\tau=0} = M(\xi - 2\xi^3 + \xi^4), \\ \left.\dfrac{\partial W}{\partial \tau}\right|_{\tau=0} = 0, \\ \Theta|_{\tau=0} = 0, \\ \left.\dfrac{\partial \Theta}{\partial \tau}\right|_{\tau=0} = 0, \end{cases} \tag{24}$$

where M is a constant relevant to the uniform force load.

Applying transformation (i.e., Eq. (22)) to Eq. (18) and Eq. (24) leads to

$$\begin{cases} \dfrac{\partial^2 W_m}{\partial \tau^2} + A_1 r_m^4 W_m - r_m^2 \Theta_m = 0, \\ (r_m^2 + A_2)\Theta_m + A_3\dfrac{\partial \Theta_m}{\partial \tau} + A_4 r_m^2 \dfrac{\partial W_m}{\partial \tau} + A_5\dfrac{\partial^2 \Theta_m}{\partial \tau^2} + A_6 r_m^2 \dfrac{\partial^2 W_m}{\partial \tau^2} = 0, \end{cases} \tag{25}$$

$$\begin{cases} W_m|_{\tau=0} = \dfrac{48}{r_m^5} M, \\ \left.\dfrac{\partial W_m}{\partial \tau}\right|_{\tau=0} = 0, \\ \Theta_m|_{\tau=0} = 0, \\ \left.\dfrac{\partial \Theta_m}{\partial \tau}\right|_{\tau=0} = 0. \end{cases} \tag{26}$$

The Laplace transformation is applied to solve Eq. (25) with regard to the initial conditions (i.e., Eq. (26)). Thus, the solution of W_m in the Laplace transformation domain can be given by

$$\widetilde{W}_m = \frac{48M(b_0 + b_1 s + b_2 s^2 + b_3 s^3)}{r_m^5 (c_0 + c_1 s + c_2 s^2 + c_3 s^3 + c_4 s^4)}, \tag{27}$$

where

$$\begin{cases} b_0 = A_4 r_m^4, \\ b_1 = r_m^4 A_6 + r_m^2 + A_2, \\ b_2 = A_3, \\ b_3 = A_5, \\ c_0 = A_1 r_m^6 + A_1 A_2 r_m^4, \\ c_1 = (A_4 + A_1 A_3) r_m^4, \\ c_2 = (A_6 + A_1 A_5) r_m^4 + r_m^2 + A_2, \\ c_3 = A_3, \\ c_4 = A_5. \end{cases} \tag{28}$$

After taking the inverse Laplace transform of Eq. (27), we can obtain the solution of W_m as

$$W_m(m,\tau) = \frac{48M}{r_m^5} \sum_{\alpha} \frac{(b_0 + b_1\alpha + b_2\alpha^2 + b_3\alpha^3)\mathrm{e}^{\alpha\tau}}{c_1 + 2c_2\alpha + 3c_3\alpha^2 + 4c_4\alpha^3}, \tag{29}$$

where α denotes the four solutions to equation $c_0 + c_1\alpha + c_2\alpha^2 + c_3\alpha^3 + c_4\alpha^4 = 0$. Thus, according to Eq. (23), the deflection can be obtained as follows:

$$W(\xi,\tau) = 2\sum_{m=1,3,\ldots}^{\infty} W_m(m,\tau)\sin(r_m\xi) = 96M \sum_{m=1,3,\ldots}^{\infty} \frac{1}{r_m^5} \sum_{\alpha} \frac{(b_0 + b_1\alpha + b_2\alpha^2 + b_3\alpha^3)\mathrm{e}^{\alpha\tau}}{c_1 + 2c_2\alpha + 3c_3\alpha^2 + 4c_4\alpha^3} \sin(r_m\xi). \tag{30}$$

In terms of Eq. (30), we can analyze the effect of thermoelastic coupling by considering a beam made of silicon $E = 169$ GPa, $\rho = 2330$ kg/m^3, $c_v = 713$ J/kg K, $\alpha_T = 2.59 \times 10^{-6}$ K^{-1}, $\nu = 0.22$ and $k = 156$ W/m K (Duwel et al., 2003). The reference temperature of the micro-beam is $T_0 = 293$ K. The aspect ratios of the beam are fixed as $L/h = 10$ and $b/h = 1/2$. When h is varied, L and b change accordingly with h. As an example, we may set such a value of the micro-beam thickness as $h/h_0 = 0.5$ ($h_0 = 20$ μm is the basic thickness used in this paper) in the calculation. Considering its first vibration mode, i.e., $m = 1$, we can get the following vibration functions:

$$\begin{aligned} W_1(1,\tau) = {} & -0.7587 \times 10^{-10}\mathrm{e}^{-1.177\times10^4\tau} + 0.1568\mathrm{e}^{-0.3049\times10^{-4}\tau}\cos(0.2850\tau) + 7.577 \times 10^{-5}\mathrm{e}^{-0.1098\tau} \\ & + 0.4598 \times 10^{-4}\mathrm{e}^{-0.3049\times10^{-4}\tau}\sin(0.2850\tau) \end{aligned} \tag{31}$$

$$\begin{aligned} \Theta_1(1,\tau) = {} & -0.1350 \times 10^{-17}\mathrm{e}^{-1.177\times10^4\tau} - 0.7158 \times 10^{-6}\mathrm{e}^{-0.3049\times10^{-4}\tau}\cos(0.2850\tau) + 0.7158 \times 10^{-6}\mathrm{e}^{-0.1098\tau} \\ & + 0.2758 \times 10^{-6}\mathrm{e}^{-0.3049\times10^{-4}\tau}\sin(0.2850\tau) \end{aligned} \tag{32}$$

Therefore, it can be found from Eqs. (31) and (32) that its nature frequency is $\Omega_1 = 0.2850$, and the dimensionless deflection, W, has the same frequency as the dimensionless thermal moment, Θ.

For a simply supported beam, if the thermoelastic damping effect is ignored, its deflection solution is

$$W_0(\xi,\tau)=\sum_{n=1,3,5,\ldots}^{\infty}\frac{96M}{n^5\pi^5}\cos\left(\frac{\sqrt{3}n^2\pi^2h}{6L}\tau\right)\sin(n\pi\xi). \tag{33}$$

The vibration frequency of the beam is

$$\Omega_0=\frac{\sqrt{3}n^2\pi^2h}{6L}. \tag{34}$$

Substituting $n=1$ into Eq. (34) gives its nature frequency of $\Omega_0=0.2849$. If h/L maintains the same value, its nature frequency is a constant.

Fig. 1 is the dynamic midspan deflection of the simply supported beam with the thickness of $h/h_0=0.5$ for the coupled thermoelastic case. It can be seen from Eq. (31) that the vibration of the beam decays with time increasing when the coupling between the strain and temperature fields is taken into account, while a steady state mode of vibration is established when the coupling is ignored. Since the vibration of the micro-beam weakens so slowly that it is hardly distinguished from the curve in Fig. 1, the difference between W and W_0 is shown in Fig. 2 to see the vibration decay caused by thermoelastic damping. Fig. 3 shows the midspan thermal moment of the simply supported beam with the thickness of $h/h_0=0.5$ for the coupled thermoelastic

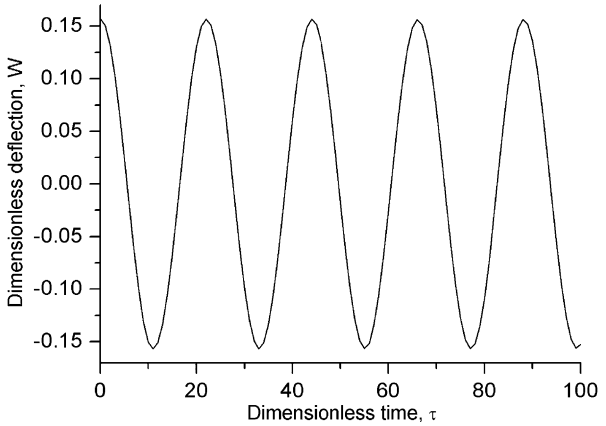

Fig. 1. Dimensionless dynamic midspan deflection of the simply supported beam with the thickness of $h/h_0=0.5$ for the coupled thermoelastic case.

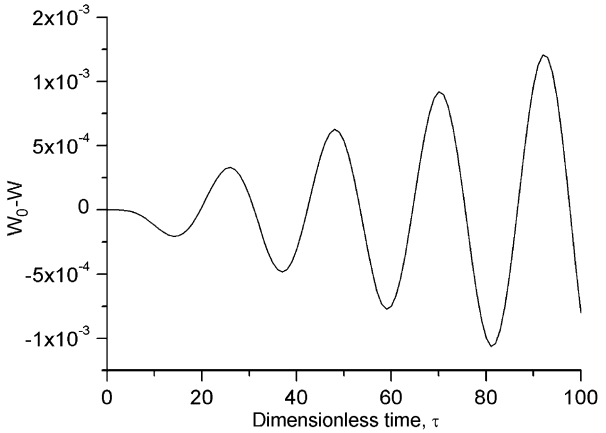

Fig. 2. The deflection difference (W_0-W) of the uncoupled and coupled cases for the simply supported beam with the thickness of $h/h_0=0.5$.

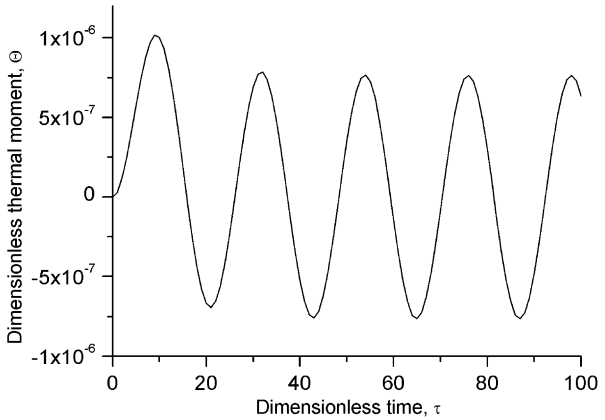

Fig. 3. Dimensionless midspan thermal moment of the simply supported beam with the thickness of $h/h_0 = 0.5$ for the coupled thermoelastic case.

case. It can be found from Fig. 3 that the decay of the dimensionless thermal moment is significant. Figs. 1–3 indicate that the deflection vibrates in a quasi-steady state mode while the thermal moment exhibits a jump at the beginning and then reaches its quasi-steady state mode of vibration quickly.

Fig. 2 shows that the amplitude of $W_0 - W$ increases quickly, that is, the amplitude of W decreases. This means that the mechanical energy of the beam is dissipated. Note that the time range in Fig. 1 is small. In fact, the attenuation of W is significant in the longer time duration. The small inset plot in Fig. 4 shows the dynamic midspan deflection of the simply supported beam with the thickness of $h/h_0 = 0.5$ during a dimensionless time range of $\tau = 0$–20,000. Indeed, the deflection amplitude exhibits considerable attenuation in a long time range. The calculated results show that the attenuation of W changes with the change of the beam thickness. Fig. 4 gives the envelope curves of dimensionless deflection for beams with different thickness ($h/h_0 = 0.1$, $h/h_0 = 0.2$, $h/h_0 = 0.5$, $h/h_0 = 2.0$) in the dimensionless time range of $\tau = 0$–2×10^4. From the envelope curves, we can draw a conclusion that when the size of the thickness decreases, the deflection amplitude attenuation increases, which means that the effect of thermoelastic damping enhances.

The characteristic time (τ_R) for heat flux to reach equilibrium was defined by Zener (1937, 1938) as given in Eq. (1). When $\tau_R = \omega^{-1}$ (the vibration frequency, ω, is given in Eq. (2)), the attenuation reaches the maximum, and we can get the characteristic thickness from this expression. In this paper, we discuss silicon beams with the aspect ratios fixed as $L/h = 10$ and $b/h = 1/2$. Thus, the characteristic thickness for the beam with both

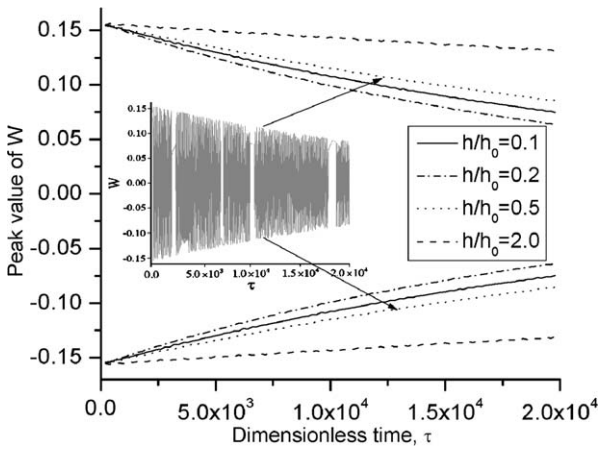

Fig. 4. Envelope curves of dimensionless deflection for micro-beams with different thickness values ($\tau = 0$–2×10^4). Inset plot: dynamic midspan deflection of the simply supported beam with the thickness of $h/h_0 = 0.5$ ($\tau = 0$–20,000).

ends simply supported is $h_{cs} = 3.819$ μm. When the thickness of the beam gets larger, $\tau_R > \omega^{-1}$, and the vibration of the micro-beam inclines to the adiabatic condition and energy dissipation becomes smaller. As an example, the case of micro-beams with both ends simply supported is examined. It can be seen from the envelope curves for different thickness values in Fig. 4 that the curve of $h/h_0 = 0.2$ declines most significantly. In the other word, when the thickness, h, reaches its characteristic thickness, the attenuation becomes stronger as shown in Fig. 4. Therefore, it may be concluded that when the thickness of the micro-beam is larger than its characteristic size, the effect of thermoelastic damping weakens as the beam thickness increases.

Fig. 5 shows the vibration response of dimensionless thermal moment Θ for beams with different thickness values in the dimensionless time range of $\tau = 0$–100. Comparing with the vibration deflection, the vibration response of thermal moment Θ is more significant. Fig. 6 illustrates the envelope curves of dimensionless thermal moment Θ for beams with different thickness values in a longer dimensionless time range of $\tau = 0$–1×10^5.

Fig. 5 demonstrates that the thermal moment curve has a jump in the beginning and then reaches quasi-steady vibration quickly. Fig. 6 indicates that after longer time, the thermal moment attenuates significantly. The thermal moment vibration curves vary with the change of thickness in different time ranges. The jump varies with the change of thickness. When the thickness decreases, the jump decreases, and the beam need less time to reach quasi-steady state of vibration.

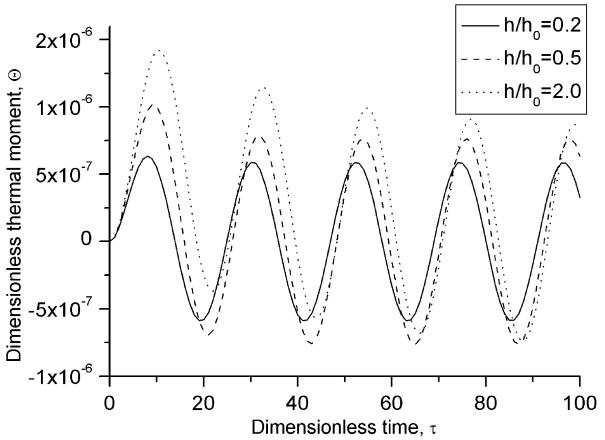

Fig. 5. Dimensionless midspan thermal moment Θ for micro-beams with different thickness values ($\tau = 0$–100).

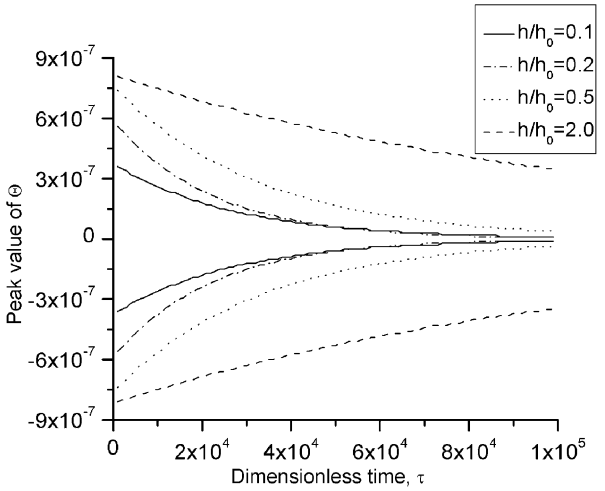

Fig. 6. Envelope curves of dimensionless thermal moment Θ for micro-beams with different thickness values ($\tau = 0$–1×10^5).

When a resonator is driven into vibration externally, the energy is dissipated and transferred from this mode to other degrees of freedom or into the environment. When an initial displacement is applied to an elastic beam, the beam will vibrate, and the vibration amplitude will attenuate with time, due to the thermoelastic coupling effect. The dissipated energy is transferred from a particular mode of the resonator, which is driven externally, to energy reservoirs formed by all the other degrees of freedom of the system. In this paper, the energy change is represented by means of both the attenuation of the deflection amplitude and the variation of the thermal moment. The amount of the mechanical energy dissipation caused by thermoelastic damping can be expressed in terms of the internal friction, Q^{-1} (Zener, 1937; Lifshitz and Roukes, 2000). According to Zener's theory (1937,1938a, 1938b), Q^{-1} decreases as the beam size increases when the beam's thickness is larger than the characteristic size. According to the result of Manolis and Beskos (1980), when the internal friction increases, the vibration attenuation induced by thermoelastic damping increases and the nature frequency increases. In the next section, therefore, we will concentrate on analyzing the size effect of vibration frequency due to thermoelastic damping.

4.2. Normal mode analysis

The normal mode analysis is applied in this section to analyze the vibration frequency shift relative to thermoelastic damping for three boundary cases, such as the clamped and isothermal, the simply supported and isothermal, and the simply supported and adiabatic at the two ends of the micro-beams. The analysis is limited to the vibration frequency characteristics due to the length of the paper. At first, we consider such a case that the two ends are clamped and isothermal. The boundary conditions are given by

$$\begin{cases} W|_{\xi=0} = W|_{\xi=1} = 0, \\ \left.\dfrac{\partial W}{\partial \xi}\right|_{\xi=0} = \left.\dfrac{\partial W}{\partial \xi}\right|_{\xi=1} = 0, \\ \Theta|_{\xi=0} = \Theta|_{\xi=1} = 0. \end{cases} \tag{35}$$

Because it is difficult to separate the variables in this case, we employ the normal mode analysis to solve the governing equations and analyze its frequency characteristics (Guo and Rogerson, 2003). The calculations in the previous section show that deflection, W, and thermal moment, Θ, vibrate in the same frequency. Therefore, both quantities change harmonically (Guo and Rogerson, 2003), i.e.,

$$\begin{cases} W = W(\xi)\mathrm{e}^{\mathrm{i}\Omega\tau}, \\ \Theta = \Theta(\xi)\mathrm{e}^{\mathrm{i}\Omega\tau}, \end{cases} \tag{36}$$

where Ω is the dimensionless frequency. We expect to find that in general the frequencies are complex, the real part $\mathrm{Re}(\Omega)$ giving the new eigenfrequencies of the beam in the presence of thermoelastic coupling effect, and the imaginary part $|\mathrm{Im}(\Omega)|$ giving the attenuation of the vibration.

Substituting Eq. (36) into Eq. (18) gives

$$-\Omega^2 W(\xi) + A_1 W^{(4)}(\xi) + \Theta''(\xi) = 0, \tag{37a}$$

$$\Theta''(\xi) - (A_2 + \mathrm{i}\Omega A_3 - A_5\Omega^2)\Theta(\xi) + (\mathrm{i}\Omega A_4 - A_6\Omega^2)W''(\xi) = 0. \tag{37b}$$

Elimination of $\Theta''(\xi)$ from Eqs. (37a) and (37b) results in

$$\Theta(\xi) = (\Omega^2 W + (\mathrm{i}\Omega A_4 - A_6\Omega^2)W'' - A_1 W^{(4)})/(A_2 + \mathrm{i}\Omega A_3 - A_5\Omega^2). \tag{38}$$

Substituting Eq. (38) into Eq. (37a) gives

$$a_1 W^{(6)}(\xi) + a_2 W^{(4)}(\xi) + a_3 W^{(2)}(\xi) + a_4 W(\xi) = 0, \tag{39}$$

where

$$\begin{cases} a_1 = A_1/(A_2 + \mathrm{i}\Omega A_3 - A_5\Omega^2), \\ a_2 = -(A_1 + (\mathrm{i}\Omega A_4 - A_6\Omega^2)/(A_2 + \mathrm{i}\Omega A_3 - A_5\Omega^2)), \\ a_3 = -\Omega^2/(A_2 + \mathrm{i}\Omega A_3 - A_5\Omega^2), \\ a_4 = \Omega^2. \end{cases} \tag{40}$$

Then the solution of dimensionless deflection $W(\xi)$ is given by

$$W(\xi) = \sum_{i=1}^{3}(B_i \sinh(\lambda_i \xi) + C_i \cosh(\lambda_i \xi)), \tag{41}$$

where, $\pm\lambda_i$, $i = 1, 2, 3$, are the roots of equation $a_1\lambda^6 + a_2\lambda^4 + a_3\lambda^2 + a_4\lambda = 0$, and B_i, C_i are constants.

Since we have got the deflection, we can substitute Eq. (41) into Eq. (38) to get the solution of the thermal moment $\Theta(\xi)$:

$$\Theta(\xi) = \sum_{i=1}^{3}(d_i B_i \sinh(\lambda_i \xi) + d_i C_i \cosh(\lambda_i \xi)) \tag{42}$$

in which

$$d_i = (\Omega^2 + (\mathrm{i}\Omega A_4 - A_6\Omega^2)\lambda_i^2 - A_1\lambda_i^4)/(A_2 + \mathrm{i}\Omega A_3 - A_5\Omega^2). \tag{43}$$

Substitute Eqs. (41) and (42) into the boundary conditions, i.e., Eq. (35), we have

$$\begin{cases} \sum_{i=1}^{3} C_i = 0, \\ \sum_{i=1}^{3}(B_i \sinh(\lambda_i) + C_i \cosh(\lambda_i)) = 0, \\ \sum_{i=1}^{3} \lambda_i B_i = 0, \\ \sum_{i=1}^{3}(\lambda_i B_i \cosh(\lambda_i) - \lambda_i C_i \sinh(\lambda_i)) = 0, \\ \sum_{i=1}^{3} d_i C_i = 0, \\ \sum_{i=1}^{3}(d_i B_i \sinh(\lambda_i) + d_i C_i \cosh(\lambda_i)) = 0. \end{cases} \tag{44}$$

In order to get non-trivial solutions, the constants B_i and C_i must be non-zero. Therefore, we obtain the following frequency equation:

$$\begin{vmatrix} 0 & 1 & 0 & 1 & 0 & 1 \\ \sinh(\lambda_1) & \cosh(\lambda_1) & \sinh(\lambda_2) & \cosh(\lambda_2) & \sinh(\lambda_3) & \cosh(\lambda_3) \\ \lambda_1 & 0 & \lambda_2 & 0 & \lambda_3 & 0 \\ \lambda_1 \cosh(\lambda_1) & \lambda_1 \sinh(\lambda_1) & \lambda_2 \cosh(\lambda_2) & \lambda_2 \sinh(\lambda_2) & \lambda_3 \cosh(\lambda_3) & \lambda_3 \sinh(\lambda_3) \\ 0 & d_1 & 0 & d_2 & 0 & d_3 \\ d_1 \sinh(\lambda_1) & d_1 \cosh(\lambda_1) & d_2 \sinh(\lambda_2) & d_2 \cosh(\lambda_2) & d_3 \sinh(\lambda_3) & d_3 \cosh(\lambda_3) \end{vmatrix} = 0. \tag{45}$$

The dimensionless frequency Ω may be obtained through solving Eq. (45).

Note that if the thermoelastic coupling effect is ignored, the dimensionless vibration frequency of the beam with both ends clamped can be expressed as

$$\Omega_0 = \frac{\sqrt{3}\beta_i^2 h}{6L} \tag{46}$$

where β_i is the ith positive root of equation $\cos(x)\cosh(x) = 1$, and its first three values are 4.730, 7.853, 10.996, respectively.

Now we analyze the frequency variation with the change of thickness of the micro-beam, h. In order to verify the validity of the analytical solution of Eq. (45), we also numerically solve Eq. (18) using the finite difference method directly and compare the numerical results with the analytical results of Eq. (45). Comparisons are made with the analytic results of the coupled normal mode theory and with the numerical results calculated directly from using the finite difference method.

Fig. 7 illustrates the change of the dimensionless first-mode frequency with the change of thickness of the beam. The beam thickness varies from $h/h_0 = 0.1$ to $h/h_0 = 1.0$, which is larger than its characteristic thickness (for a beam clamped at both ends, the characteristic length is $h_{cc} = 1.685$ μm). According to the analysis in Section 4.1, the vibration frequency of the beam will decrease as the dimension of the beam increases, as is presented in Fig. 7. To see the scale effect, the vibration frequency of the uncoupled thermoelastic problem is also presented in Fig. 7 as the solid-square marked horizontal line. The results of coupled thermoelastic problems conclude the analytic results of Eq. (45) and the numerical results of Eq. (18) via the finite difference method.

Fig. 7 shows that the analytic results of Eq. (45) are in good agreement with the numerical results of Eq. (18), and the difference between the two methods decreases as the thickness of the beam increases. When the thickness of the beam increases to $h/h_0 = 1.0$, they are almost of the same value. Fig. 7 demonstrates that the dimensionless frequency is size-dependent when the effect of thermoelastic coupling is considered. This is because the coefficients A_3 and A_4 in the dimensionless Eq. (18) are size-dependent. In contrast, the dimensionless frequency only depends upon the ratio of thickness to length as shown in Eq. (45) when the thermoelastic coupling effect is disregarded. From the curves in Fig. 7 we can see that the thermoelastic coupling generally shifts the vibration frequency and this effect increases as the thickness of the micro-beam decreases. However, the decreasing rate of the vibration frequency (i.e., the slop of the curve) declines considerably as the beam thickness increases. When the thickness of the micro-beam reaches a critical value (say over 20 μm for a given silicon material and at the specified boundary condition), the curve is close to the horizontal line corresponding to the uncoupled thermoelastic problem. Note that the slope of the curve is close to zero after the beam thickness is over the critical value. It may be expected, therefore, that the size-effect induced by thermoelastic coupling would disappear when the thickness of the micro-beam reaches a critical value that is not a universal constant, but depends on the material properties and the boundary conditions.

To give a summarization, we need to analyze frequencies of micro-beams with different boundary conditions.

When the two ends of the beam are simply supported and isothermal, the boundary conditions are shown in Eq. (21). Substituting expressions of deflection and thermal moment, i.e., Eqs. (41) and (42), into the boundary conditions (i.e., Eq. (21)), yields the following frequency equation:

$$\begin{vmatrix} 0 & 1 & 0 & 1 & 0 & 1 \\ \sinh(\lambda_1) & \cosh(\lambda_1) & \sinh(\lambda_2) & \cosh(\lambda_2) & \sinh(\lambda_3) & \cosh(\lambda_3) \\ 0 & \lambda_1^2 & 0 & \lambda_2^2 & 0 & \lambda_3^2 \\ \lambda_1^2\sinh(\lambda_1) & \lambda_1^2\cosh(\lambda_1) & \lambda_2^2\sinh(\lambda_2) & \lambda_2^2\cosh(\lambda_2) & \lambda_3^2\sinh(\lambda_3) & \lambda_3^2\cosh(\lambda_3) \\ 0 & d_1 & 0 & d_2 & 0 & d_3 \\ d_1\sinh(\lambda_1) & d_1\cosh(\lambda_1) & d_2\sinh(\lambda_2) & d_2\cosh(\lambda_2) & d_3\sinh(\lambda_3) & d_3\cosh(\lambda_3) \end{vmatrix} = 0. \tag{47}$$

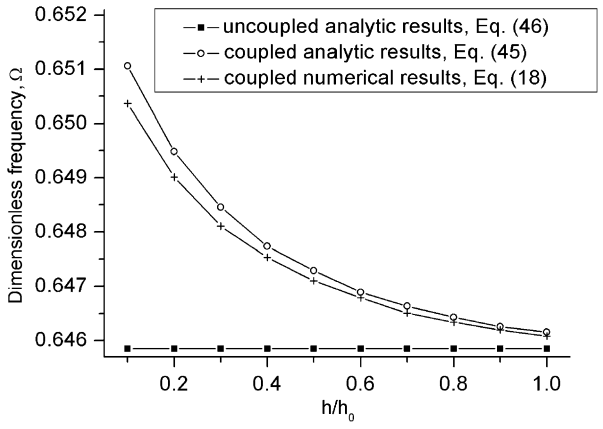

Fig. 7. Variation of the dimensionless natural frequency with the change of thickness of the beam ($h_0 = 20$ μm).

Table 1
Frequency shift ratio via beam thickness for micro-beams with three boundary conditions: (a) both ends simply supported and isothermal; (b) both ends simply supported and adiabatic; (c) both ends clamped and isothermal ($h_0 = 20$ μm)

h/h_0	Frequency shift ratio, $(\Omega - \Omega_0)/\Omega_0$ ($\times 10^{-4}$)		
	$\Omega_0 = 0.2849$	$\Omega_0 = 0.2849$	$\Omega_0 = 0.6458$
0.2	6.864	6.697	56.25
0.5	2.775	2.708	22.30
1.0	0.5898	0.5587	4.703

When the two ends of the beam are simply supported and adiabatic, the boundary conditions become

$$\begin{cases} W|_{\xi=0} = W|_{\xi=1} = 0, \\ \left.\dfrac{\partial^2 W}{\partial \xi^2}\right|_{\xi=0} = \left.\dfrac{\partial^2 W}{\partial \xi^2}\right|_{\xi=1} = 0, \\ \dfrac{\partial \Theta}{\partial \xi}|_{\xi=0} = \dfrac{\partial \Theta}{\partial \xi}|_{\xi=1} = 0. \end{cases} \tag{48}$$

Substituting Eqs. (41) and (42) into the boundary conditions (i.e., Eq. (48)) gives

$$\begin{vmatrix} 0 & 1 & 0 & 1 & 0 & 1 \\ \sinh(\lambda_1) & \cosh(\lambda_1) & \sinh(\lambda_2) & \cosh(\lambda_2) & \sinh(\lambda_3) & \cosh(\lambda_3) \\ 0 & \lambda_1^2 & 0 & \lambda_2^2 & 0 & \lambda_3^2 \\ \lambda_1^2 \sinh(\lambda_1) & \lambda_1^2 \cosh(\lambda_1) & \lambda_2^2 \sinh(\lambda_2) & \lambda_2^2 \cosh(\lambda_2) & \lambda_3^2 \sinh(\lambda_3) & \lambda_3^2 \cosh(\lambda_3) \\ d_1\lambda_1 & 0 & d_2\lambda_2 & 0 & d_3\lambda_3 & 0 \\ d_1\lambda_1 \cosh(\lambda_1) & d_1\lambda_1 \sinh(\lambda_1) & d_2\lambda_2 \cosh(\lambda_2) & d_2\lambda_2 \sinh(\lambda_2) & d_3\lambda_3 \cosh(\lambda_3) & d_3\lambda_3 \sinh(\lambda_3) \end{vmatrix} = 0. \tag{49}$$

The vibration frequencies under the two boundary conditions can be obtained by solving Eqs. (47) and (49), respectively. Table 1 shows frequency shift ratio $(\Omega - \Omega_0)/\Omega_0$ under three kinds of boundary conditions, where Ω_0 is the dimensionless frequency of the uncoupled problems.

Table 1 shows the effect of the boundary conditions on frequency shift ratio. The frequency shift ratio for beams with both ends clamped is a little larger, and on the order of 10^{-3}. While for beams with both ends simply supported, the frequency shift ratio is on the order of 10^{-4}. It is interesting to notice from the table that the frequency shift ratio is higher for beams with both ends isothermal than that for beams with both ends adiabatic.

5. Discussion

Zhang et al. (2003) analyzed the air damping effect on the damping ratio and resonant frequency shift ratio of beams with both ends clamped. The damping ratio obtained by them is

$$\zeta_1 = \frac{a\mu L^2}{h^2 b q^2}\sqrt{\frac{3}{E\rho}}. \tag{50}$$

The shift ratio of the resonant frequency was given by them as follows:

$$\Delta\omega = \frac{p_1 - \omega_1}{p_1} = 1 - \sqrt{1 - 2\zeta_1^2}, \tag{51}$$

where $q = 4.73$, a is a constant related to Reynolds number, and μ is the dynamic viscosity of the air.

Zhang et al. (2003) gave the parameters as $a = 10$ and $\mu = 1.81 \times 10^{-5}$ N s/m^2. For a beam with the thickness of $h = 10$ μm and both ends clamped, substituting these parameters into Eqs. (50) and (51) yields the values: $\zeta_1 = 1.412 \times 10^{-5}$, $\Delta\omega = 2 \times 10^{-10}$.

However, in our calculation, the corresponding values are $\zeta_1 = 3.276 \times 10^{-5}$, $\Delta\omega = 2.230 \times 10^{-3}$. These results indicate that the effect of thermoelastic damping is larger than the effect of air damping for micro-beam resonators at room temperature. The effect of air damping is affected by the changes of environment. For example, it can be minimized under ultrahigh-vacuum (UHV) conditions. While thermoelastic damping is an intrinsic dissipation mechanism and will not be affected by the changes of environment. Therefore, it is more important to study the effect of thermoelastic damping on the mechanical behavior of MEMS.

We have made some simplifications and assumptions that would be summarized here.

(1) The usual Euler–Bernoulli assumption for a thin beam undergoing small flexural vibrations is made. Our results do not hold for large amplitude vibrations, where non-linear behavior begins to take over. Besides, they do not hold for thick and short beams, for which the Timoshenko assumption should be considered.
(2) In this study, the general coupled thermoelastic formulation is adapted, which is based on the continuum theory frame. Therefore, the whole analysis relative to thermoelastic damping for the micro-beam resonators does not involve in any micro-mechanisms. This is because the phonon mean free path (about 20–100 nm) is much smaller than the geometric length of the micro-beams (i.e., at the scale of micron), and the system remains in the diffusive regime. If the thickness of the beam is decreased until into the nanometer scale, the phonon mean free path becomes comparable to the beam thickness, where the transport of thermal energy crosses over from being diffusive to being ballistic, and other formulations should be used.
(3) The material's thermal expansion coefficient α_T is expressed as $\alpha_T = (1/L)\partial L/\partial T$. From its expression, we can see that it is temperature dependent. Under low temperature, α_T is small and the thermoelastic damping is no longer significant, but it is an important mechanism of energy dissipation at room temperature.
(4) The material's thermal expansion coefficient α_T also depends on the size of the beam. Since we use a constant value of α_T in the present study for simplification, there exist some errors in the calculations. Nevertheless, main characteristics relative to the effects of thermoelastic damping on the vibration behavior of the micro-beam resonators can still be captured.

6. Conclusions

This paper analyzes the effect of thermoelastic coupling on deflection amplitudes, thermal moment amplitudes as well as vibration frequencies and proves that thermoelastic damping is a significant loss mechanism at room temperature for micro-scale beam resonators.

Given the same initial displacement, beams in smaller size experience larger volume change and higher temperature gradient, which lead to more energy dissipation, namely faster attenuation of the vibration amplitude. That is, the thermoelastic damping of micro-beam resonators exhibits obvious size effect. The results indicate that the deflection and the thermal moment vibrate in the same frequency. For the thermal moment, there exists a jump at the beginning, and then it reaches a quasi-steady vibration state. In a long time range, both the dimensionless deflection and the thermal moment attenuate with time obviously. The thermoelastic damping process is affected by the supporting and heat transfer conditions at the two ends of the micro-beam. The calculated results show that the frequency shift ratio is on the order of 10^{-3} for beams with the two ends clamped, while it is on the order of 10^{-4} for beams with the two ends simply supported. Furthermore, the frequency shift ratio for beams with the two ends held at constant temperature is higher than that for beams with the two ends adiabatic.

Both the analytic and the numerical results indicate that the dimensionless frequency is scale-dependent with thermoelastic coupling being considered. When the thickness, h, reaches its characteristic thickness, the vibration attenuation of the micro-beam becomes stronger. That is, when the thickness of the micro-beam is larger than its characteristic size, the effect of thermoelastic damping weakens as the beam thickness increases.

Comparing to air damping, the results demonstrate that the effect of thermoelastic damping is larger than the effect of air damping for micro-beam resonators at room temperature. Since thermoelastic damping is an intrinsic dissipation mechanism and will not be affected by the changes of environment, it is more important to study the effect of thermoelastic damping on the mechanical behavior of MEMS.

Acknowledgments

The authors are grateful for the support by National Natural Science Foundation of China under Grants #90208002, #90305015. Support from the Research Grants Council of the Hong Kong Special Administrative Region, China (project no. HKU 7195/04E) is acknowledged also.

References

Akhiezer, A.I., Berestetskii, V.B., 1965. Quantum Electrodynamics. Interscience Publishers, New York.
Barnes, J.R., Stephenson, R.J., Welland, M.E., Gerber, C.H., Gimzewski, J.K., 1994. Photothermal spectroscopy with femtoJoule sensitivity using a micromechanical device. Nature 372, 79–81.
Berry, B.S., 1955. Precise investigation of the theory of damping by transverse thermal currents. J. Appl. Phys. 26, 1221–1224.
Boley, B.A., 1972. Approximate analyses of thermally induced vibrations of beams and plates. J. Appl. Mech. 39, 212–216.
Burns, D.W., Zook, J.D., Horning, R.D., Herb, W.R., Guckel, H., 1995. Sealed-cavity resonant microbeam pressure sensor. Sensors Actuat. A 48, 179–186.
Carr, D.W., Sekaric, L., Craighead, H.G., 1998. Measurement of nanomechanical resonant structures in single-crystal silicon. J. Vac. Sci. Technol. B 16, 3821–3824.
Cleland, A.N., Roukes, M.L., 1996. Fabrication of high frequency nanometer scale mechanical resonators from bulk Si crystals. Appl. Phys. Lett. 69, 2653–2655.
Cleland, A.N., Roukes, M.L., 1999. External control of dissipation in a nanometer-scale radio frequency mechanical resonator. Sensors Actuat. A 72, 256–261.
Copper, C.D., Pilkey, W.D., 2002. Thermoelasticity solutions for straight beams. Trans. ASME, J. Appl. Mech. 69, 224–229.
Duwel, A., Gorman, J., Weinstein, M., Borenstein, J., Ward, P., 2003. Experimental study of thermoelastic damping in MEMS gyros. Sensors Actuat. A 103, 70–75.
Ezzat, M.A., Othman, M.I., EI-Karamany, A.S., 2001. Electromagneto-thermoelastic plane waves with thermal relaxation in a medium of perfect conductivity. J. Thermal Stresses 24, 411–432.
Givoli, D., Rand, O., 1995. Dynamic thermoelastic coupling effects in a rod. AIAA J. 33 (4), 776–778.
Guo, F.L., Rogerson, G.A., 2003. Thermoelastic coupling effect on a micro-machined beam machined beam resonator. Mech. Res. Commun. 30, 513–518.
Harrington, D.A., Mohanty, P., Roukes, M.L., 2000. Energy dissipation in suspended micromechanical resonators at low temperatures. Physica B 284–288, 2145–2146.
Hosaka, H., Itao, K., Kuroda, K., 1995. Damping characteristics of beam-shaped micro-oscillators. Sensors Actuat. A 49, 87–95.
Houston, B.H., Photiadis, D.M., Vignola, J.F., Marcus, M.H., Xiao, Liu, Czaplewski, D., Sekaric, L., Butler, J., Pehrsson, P., Bucaro, J.A., 2004. Loss due to transverse thermoelastic currents in microscale resonators. Mater. Sci. Eng. A 370, 407–411.
Landau, L.D., Lifshitz, E.M., 1959. Theory of Elasticity. Pergamon Press, Oxford.
Lifshitz, R., Roukes, M.L., 2000. Thermoelastic damping in micro- and nanomechanical systems. Phys. Rev. B 61, 5600–5609.
Manolis, G.D., Beskos, D.E., 1980. Thermally Induced vibrations of beam structures. Comput. Meth. Appl. Mech. Eng. 21, 337–355.
Massalas, C.V., Kalpakiclis, V.K., 1983. Coupled thermoelastic vibrations of a simply supported beam. J. Sound Vibr. 88 (3), 425–429.
Mihailovich, R.E., MacDonald, N.C., 1995. Dissipation measurements of vacuum-operated single-crystal silicon microresonators. Sensors Actuat. A 50, 199–207.
Mihailovich, R.E., Parpia, J.M., 1992. Low temperature mechanical properties of boron-doped silicon. Phys. Rev. Lett. 68, 3052–3055.
Roszhardt, R.V., 1990. The effect of thermoelastic internal friction on the Q of micromachined silicon resonators. IEEE Solid State Sensor and Actuator Workshop, Hilton Head Island, SC, USA, June, pp.13–16.
Stowe, T., Yasumura, K., Kenny, T., Botkin, D., Wago, K., Rugar, D., 1996. Ultrasensitive vertical force probe for magnetic resonance force microscopy. Solid-State Sensor and Actuator Workshop, Hilton Head, SC, USA, June 2–6, pp. 225–230.
Tang, W.C., Nguyen, T.C.H., Judy, M.W., Howe, R.T., 1990. Electrostatic-comb drive of lateral polysilicon resonators. Sensors Actuat. A 21, 328–331.
Tilmans, H.A.C., Blwenspoek, M., Fluitman, J.H.J., 1992. Micro resonator force gauges. Sensors Actuat. A 30, 35–53.
Tortonese, M., Barrett, R.C., Quate, C.F., 1993. Atomic resolution with an atomic force microscope using piezoresistive detection. Appl. Phys. Lett. 62, 834–836.
Yasumura, K.Y., Stowe, T.D., Kenny, T.W., Rugar, D., 1999. Bull. Am. Phys. Soc. 44 (1), 540.
Yurke, B., Greywall, D.S., Pargellis, A.N., Busch, P.A., 1995. Theory of amplifier-noise evasion in an oscillator employing a nonlinear resonator. Phys. Rev. A 51, 4211–4229.
Zener, C., 1937. Internal friction in solids. I. Theory of internal friction in reeds. Phys. Rev. 52, 230–235.

Zener, C., 1938. Internal friction in solids. II. General theory of thermoelastic internal friction. Phys. Rev. 53, 90–99.
Zener, C., Otis, W., Nuckolls, R., 1938. Internal friction in solids. III. Experimental demonstration of thermoelastic internal friction. Phys. Rev. 53, 100–101.
Zhang, C., Xu, G., Jiang, Q., 2003. Analysis of the air-damping effect on a micromachined beam resonator. Math. Mech. Solids 8, 315–325.
Zook, D., Burns, W., Herb, R., Guckel, H., Kang, W., Ahn, Y., 1996. Optically excited self-resonant microbeams. Sensors Actuat. A 52, 92–98.